Journal of Computational Physics 228 (2009) 8467–8479

Contents lists available at ScienceDirect

Journal of Computational Physics

journal homepage: www.elsevier.com/locate/jcp

Local stress calculation in simulations of multicomponent systems

Paulo S. Branicio *, David J. Srolovitz

Materials Theory and Simulation Laboratory, Institute of High Performance Computing, 1 Fusionopolis Way, 16-16 Connexis, Singapore 138632, Singapore

ARTICLE INFO

Article history:
Received 23 February 2009
Received in revised form 21 August 2009
Accepted 26 August 2009
Available online 1 September 2009

PACS:
61.43.Bn
02.70.Ns
46.40.Cd
83.85.St

Keywords:
Molecular dynamics
Local stress
Localization function
Virial stress
Cauchy stress
Shock waves

ABSTRACT

The virial and Hardy methods provide accurate local stresses for single component materials such as monatomic metals. In contrast to the elemental material case, both methods provide poor estimates of the local stress for multicomponent materials. Using binary materials such as CaO, SiC and AlN and homogeneous strain, we demonstrate that there are several sources for the slow convergence of the virial and Hardy local stresses to the bulk values. Different approaches such as enforced stoichiometry, atomic localization functions and the atomic voronoi volume are used to improve the convergence and increase the spatial resolution of the local stress. The virial method with enforced stoichiometry and atomic voronoi volumes is the most accurate, giving exact stress values by the first atomic shell. In the general case, not assuming stoichiometry, the virial method with localization functions converge to 93% of the bulk value by the third atomic shell. This work may be particularly useful for the real-time description of stresses in simulations of shock waves and deformation dynamics.

1. Introduction

The local stress field quantifies the microscopic deformation state in solids. In atomistic simulations, the local stress field can be used to locate individual defects and characterize their structure and dynamics under arbitrary loading conditions. In molecular dynamics (MD) simulations, local stresses have been useful in the analysis of a wide range of phenomena such as film growth [1], shock loading [2–4], dislocation dynamics [5,6], and semiconductor nanopixel relaxation [7,8].

The most common definition of stress used with MD simulations originates from the Virial theorem developed by Clausius [9] and Maxwell [10,11]. Because of its ease of implementation and relatively low computational demands, the virial stress can be computed directly in the main loop in an MD simulation code using the interaction forces between pairs of atoms that are already calculated. Because of its computational convenience, the most widely used definition of local stress is the atomic virial, which is calculated at every atomic position and averaged to give the system or mean stress. Although the virial stress expression can be shown to be rigorous only as an ensemble average over an entire system in thermodynamic equilibrium, the atomic virial has been widely used as a measure of local stress, even in systems far from equilibrium. Nevertheless, the virial stress has been shown to lead to erroneous results in some special cases, such as close to a free surface [12,13].

Instead of starting from the definition of an ensemble average stress, Hardy derived an expression for the local stress, as well as for the local heat flux, from the definition of local mass and momentum density and the continuity equations for

* Corresponding author.
E-mail address: branicio@ihpc.a-star.edu.sg (P.S. Branicio).

0021-9991/$ - see front matter © 2009 Elsevier Inc. All rights reserved.
doi:10.1016/j.jcp.2009.08.024

mass, momentum, and energy conservation [14]. The expression for the local stress resembles the Lutsko expression [15] and also that derived by Irving and Kirkwood [16]. However, it requires that densities and fluxes exactly satisfy local, continuum conservation laws. One of the advantages of the Hardy approach is the arbitrary choice of localization function and average volume to fine tune the resolution of the calculated quantities [17]. The Hardy and virial stresses have been compared for single component systems, subject to deformation and finite temperature, and the Hardy stresses were shown to converge quicker to values expected from continuum theory [18]. The original Hardy formulation assumed only two-body interatomic potentials but recently it was demonstrated by Delph [19] and Chen [20] to also be valid for arbitrary multibody interatomic potentials, thereby extending its applicability to any translational and rotational invariant interatomic potential.

The accuracy of local stress expressions was analyzed for single component systems. However, we find no thorough examinations of their applicability to multi-component systems. While ensemble averages of the stress are independent of the number of atomic components, the local stress can suffer from stoichiometric unbalance in multiple atom unit cells in small average volumes. Therefore, it is important to examine the convergence of the calculation of local stress for multicomponent systems in order to quantify their accuracy and spatial resolution.

In this paper, we discuss the calculation of the local stress for multicomponent systems based on the virial and Hardy methods. As there is no uniqueness in the calculation of local stresses, we quantify the accuracy of these approaches for different systems at different strain loads. In particular, we examine the binary systems CaO, SiC and AlN, subject to homogeneous strains to determine their convergence and computational convenience. Details of the definitions of local stress are presented in Section 2. Details of the calculation of local stress for multicomponent systems, its convergence and computational convenience are discussed in Section 3. The calculation of local density is discussed in Section 4. Finally, we discuss alternative approaches for determining the atomic-level stress in Section 5 and summarize the work in the last section of the paper.

2. Definition of local stresses

The virial stress [9–11] for a system with N atoms and total volume Ω is given by the relation

$$\Pi^{\alpha\beta} = -\frac{1}{\Omega}\sum_{i=1}^{N}\left[\frac{1}{2}\sum_{\substack{j=1\\ j\neq i}}^{N} f_{ij}^{\alpha} r_{ij}^{\beta} + m_i v_i^{\alpha} v_i^{\beta}\right], \tag{1}$$

where $\alpha, \beta = x, y, z$ indicate directions in an orthogonal, laboratory frame, m_i and v_i^{α} are the mass and the α component of the velocity of atom i. r_{ij}^{β} is the β component of the vector connecting atoms i and j, and f_{ij}^{α} is the α component of the force on atom i due to atom j. As is common in MD simulations, this expression can be rewritten as

$$\Pi^{\alpha\beta} = \frac{1}{\Omega}\sum_{i=1}^{N} \Omega_i^a \pi_i^{\alpha\beta}, \tag{2}$$

with

$$\pi_i^{\alpha\beta} = -\frac{1}{\Omega_i^a}\left[\frac{1}{2}\sum_{\substack{j=1\\ j\neq i}}^{N} f_{ij}^{\alpha} r_{ij}^{\beta} + m_i v_i^{\alpha} v_i^{\beta}\right], \tag{3}$$

where $\pi_i^{\alpha\beta}$ and Ω_i^a are the atomic virial stress and the atomic volume associated with atom i. As the fluctuations of the atomic virial stress can be large, the atomic virial stress is often averaged over a volume containing several atoms. This volume can be centered at any given $\mathbf{R}$ position, including the atomic positions, and the local virial stress is calculated using the expression

$$\pi^{\alpha\beta}(\mathbf{R}) = -\frac{1}{\Omega^c}\sum_{\substack{i=1\\ i\in\Omega^c}}^{N}\left[\frac{1}{2}\sum_{\substack{j=1\\ j\neq i}}^{N} f_{ij}^{\alpha} r_{ij}^{\beta} + m_i v_i^{\alpha} v_i^{\beta}\right], \tag{4}$$

where $\Omega^c = \frac{4}{3}\pi r_c^3$ is the spherical volume of radius r_c centered at $\mathbf{R}$.

In the Hardy formulation [14,17], the properties of each atom are spread out in space by use of a localization function $\psi(\mathbf{r}_i - \mathbf{R})$. This function should satisfy the following conditions:

1. non-negative and smooth;
2. peaked at $\mathbf{r}_i = \mathbf{R}$ and decays to zero at $|\mathbf{r}_i - \mathbf{R}| = r_c$;
3. normalized such that $\int \psi d^3\mathbf{r} = 1$.

Hardy [14] defined the mass density and momentum density using this localization function as:

$$\rho(\mathbf{R},t)=\sum_{\alpha=1}^{N} m_i\psi(\mathbf{r}_i-\mathbf{R}), \tag{5}$$

$$\mathbf{p}(\mathbf{R},t)=\sum_{\alpha=1}^{N} m_i\mathbf{v}_i\psi(\mathbf{r}_i-\mathbf{R}). \tag{6}$$

The material velocity field $\mathbf{v}(\mathbf{R},t)$ is defined such that $\mathbf{p}=\rho\mathbf{v}$. A bond function B between atoms i and j and related to ψ is defined by

$$B(\mathbf{r}_i,\mathbf{r}_j,\mathbf{R})\equiv\int_0^1 d\lambda\psi(\lambda\mathbf{r}_{ij}+\mathbf{r}_j-\mathbf{R}). \tag{7}$$

This function gives the integral of ψ along the line that connects the atoms i and j.

Using these definitions, Hardy gives the local stress as

$$\pi^{\alpha\beta}(\mathbf{R})=-\sum_{i=1}^{N}\left[\frac{1}{2}\sum_{\substack{j=1\\ j\neq i}}^{N} f_{ij}^{\alpha}r_{ij}^{\beta}B(\mathbf{r}_i,\mathbf{r}_j,\mathbf{R})+m_iu_i^{\alpha}u_i^{\beta}\psi(\mathbf{r}_i-\mathbf{R})\right], \tag{8}$$

where $u_i^{\alpha}\equiv v_i^{\alpha}-v^{\alpha}$ is the α component of the velocity of atom i minus the velocity field at the position $\mathbf{R}$.

The Hardy expression was originally derived considering two-body interatomic potentials, $\phi(r_{ij})$, such that

$$f_i^{\alpha}=\sum_{\substack{j=1\\ j\neq i}}^{N} f_{ij}^{\alpha}=-\sum_{\substack{j=1\\ j\neq i}}^{N}\frac{r_{ij}^{\alpha}}{r_{ij}}\frac{\partial\phi(r_{ij})}{\partial r_{ij}}. \tag{9}$$

However, Eq. (8) was recently shown to be valid for arbitrary multibody interatomic potentials [19,20]. It was shown that any such potential can be rewritten as a sum of a two-body term, a three body term and so on up to an N-body term, such as the multibody interatomic potential ϕ can be written as

$$\phi=\sum_i\sum_{j>i}V_2(r_{ij})+\sum_i\sum_{j>i}\sum_{k>j}V_3(r_{ij},r_{ik},r_{kj})+\cdots \tag{10}$$

Such potential only preserves the translational and rotational invariance if ϕ depends only on the squares of the interatomic distances. Therefore a three body potential can be rewritten as

$$\phi=\frac{1}{2}\sum_{i\neq j}\phi_{ij},\quad \phi_{ij}=\sum_{k\neq i,j}\phi_{ij}(r_{ij},r_{ik},r_{jk}), \tag{11}$$

which is compatible with the Hardy formulation.

3. Calculation of local stress in homogeneously strained binary systems

Here the virial and Hardy expressions are used to calculate the local stress in CaO, SiC, and AlN structures. These materials are representative of multicomponent systems as well as systems with different interatomic potentials. We model CaO using a two-body interatomic potential [21] and SiC and AlN using three-body interaction potentials [3,22]. CaO has the low pressure rock salt structure shown in Fig. 1(a). SiC is stable at low pressures in several structures. Here, we focus on the cubic

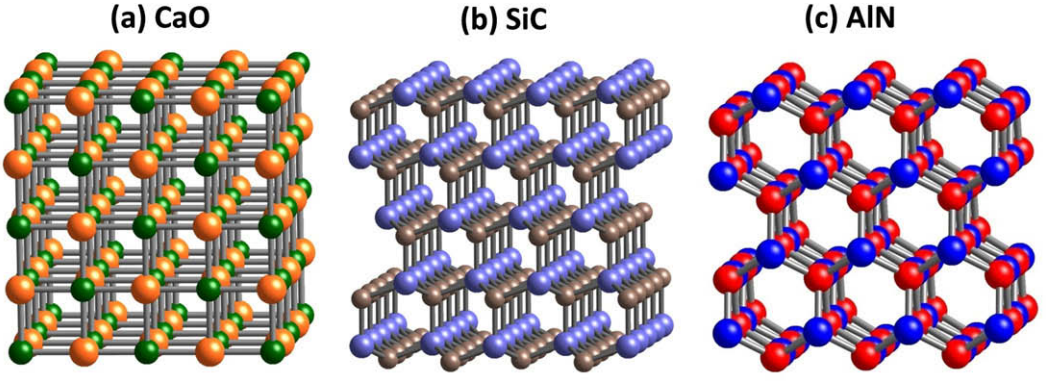

Fig. 1. Crystal structures of CaO, SiC and AlN used to investigate local stress: (a) rock salt, (b) zinc blende, and (c) wurtzite structures.

3C–SiC structure shown in Fig. 1(b). AlN is stable in the wurtzite structure at low pressure, as shown in Fig. 1(c). The accuracy of the local stress methods is estimated using a simple test case; i.e., their ability to calculate the correct stress in a homogeneous strain state. As the local stress must match the bulk stress if the sample volume is sufficiently large, the accuracy can be accessed directly by comparing the value of the calculated local stress against its bulk value for an increasing radius of the spherical average volume. The local stress is calculated under three conditions: (i) in the static, relaxed state at $T = 0$ K, for hydrostatic pressure $P = 0$ GPa; (ii) static, relaxed state at $T = 0$ K but reducing the original volume by 5%; and (iii) dynamic state at $T = 1000$ K, but constraining the volume to be the same as at $T = 0$ K (i.e., compressed).

At $T = 0$ K the crystals are static and the local stress can be calculated instantaneously from the interatomic forces. Systems are created with no strains such that all components of the bulk stress are zero. Fig. 2 shows the virial and Hardy local stresses for the CaO, SiC, and AlN structures. The Hardy stress uses a step localization function, i.e. it is constant inside of the averaging volume and is zero outsize of it. For each material the local stress is calculated at each atomic position. For CaO at both Ca and O atomic positions both the virial and Hardy stresses fluctuate as the radius of the spherical volume is increased. The fluctuation is high up to the third atomic shell at 4.1 Å with the Hardy stress fluctuation exceeding 30 GPa. Beyond this radius, the fluctuation continuously reduces but still is considerable till above ~12 Å. This extremely large fluctuation seriously compromises the determination of a meaningful local stress, especially around crystalline defects such as dislocations. The behavior of the local stresses for the SiC and AlN structures present a similar large fluctuation and slow convergence to the $P = 0$ GPa bulk stress.

At $T = 0$ K, with the volume reduced by 5%, the configuration is static and under compression. Because the structures and interatomic potentials for the three materials are different and represent different equations of state, the pressure resultant from the volume decrease is different. As shown in Fig. 3(a) and (b) for the CaO structure it is ~7 GPa. The fluctuation amplitude shown by the local stress for the relaxed structures are unchanged for the compressed state as compared with the $P = 0$ GPa state in Fig. 2. Fig. 3(c–f) show that the convergence for SiC and AlN structures is still slow and fluctuation is still noticeable even at 20 Å. With such large fluctuations the virial and Hardy stresses are unsuitable for discerning microscopic details from the local stress field since the spatial resolution suffers from slow convergence. Additionally, the reliable calculation of the stress for each atomic position is computationally costly, since it requires the consideration of all neighboring atoms enclosed in a large spherical volume.

An idea to improve the averages of the local stress for multicomponent systems is to ensure that the averaging volume contains an integer number of stoichiometric units [4]. In the case of homogeneous, multicomponent systems with no segregation the assumption of stoichiometry is reasonable. The stoichiometric virial expression for a given binary A_kB_l material is given by

$$\pi^{\alpha\beta}(\mathbf{R}) = -\frac{m+n}{(k+l)\Omega^c}\left(k\pi_A^{\alpha\beta} + l\pi_B^{\alpha\beta}\right), \tag{12}$$

where m and n are the number of A and B atoms within the spherical volume Ω^c with the partial stresses given by

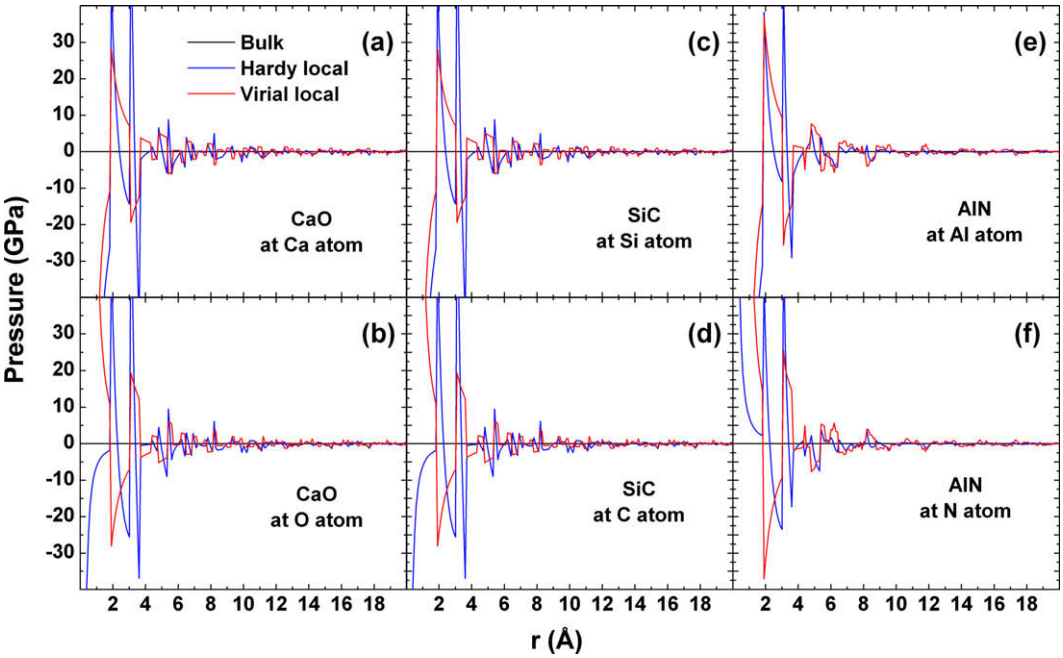

Fig. 2. Local stress calculated at $P = 0$ GPa and $T = 0$ K at different atomic positions for (a and b) CaO, (c and d) SiC and (e and f) AlN. Curves show the virial and Hardy stresses calculated in a spherical volume for increasing radius. Hardy stress is calculated using the step localization function.

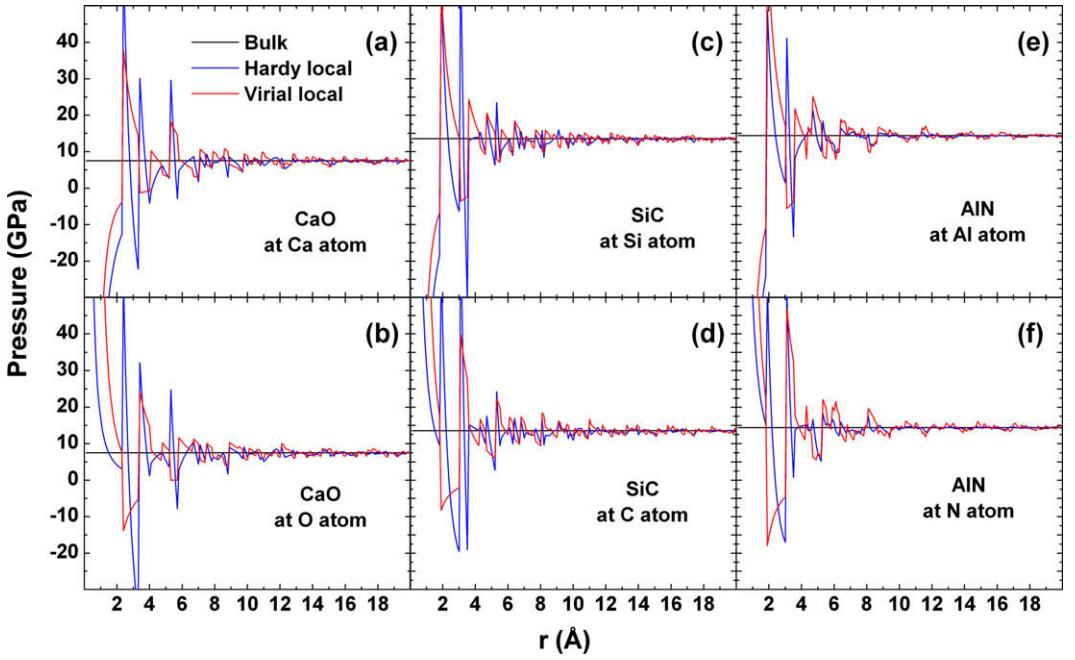

Fig. 3. Local stress calculated at $T = 0$ K and 5% volume reduction for (a and b) CaO, (c and d) SiC, and (e and f) AlN.

$$\pi_A^{\alpha\beta} = \frac{1}{m}\sum_{\substack{i=1\\ i\in\Omega^c}}^{m}\left[\frac{1}{2}\sum_{\substack{j=1\\ j\neq i}}^{N} f_{ij}^{\alpha} r_{ij}^{\beta} + m_i v_i^{\alpha} v_i^{\beta}\right]_A, \tag{13}$$

and

$$\pi_B^{\alpha\beta} = \frac{1}{n}\sum_{\substack{i=1\\ i\in\Omega^c}}^{n}\left[\frac{1}{2}\sum_{\substack{j=1\\ j\neq i}}^{N} f_{ij}^{\alpha} r_{ij}^{\beta} + m_i v_i^{\alpha} v_i^{\beta}\right]_B. \tag{14}$$

The index i refers to A atoms in Eq. (13) and to B atoms in Eq. (14), while the index j refers to all other atoms in both equations. Similar expressions for Eq. (12) can be defined for a ternary or quaternary material. The stoichiometric Hardy stress expression is similarly given by

$$\pi^{\alpha\beta}(\mathbf{R}) = -\frac{m+n}{(k+l)}\left(k\pi_A^{\alpha\beta} + l\pi_B^{\alpha\beta}\right), \tag{15}$$

with the partial stresses calculated considering only one type of species given by

$$\pi_A^{\alpha\beta} = \frac{1}{m}\sum_{i=1}^{m}\left[\frac{1}{2}\sum_{\substack{j=1\\ j\neq i}}^{N} f_{ij}^{\alpha} r_{ij}^{\beta} B(\mathbf{r}_i, \mathbf{r}_j, \mathbf{R}) + m_i u_i^{\alpha} u_i^{\beta}\psi(\mathbf{r}_i - \mathbf{R})\right]_A, \tag{16}$$

and

$$\pi_B^{\alpha\beta} = \frac{1}{n}\sum_{i=1}^{n}\left[\frac{1}{2}\sum_{\substack{j=1\\ j\neq i}}^{N} f_{ij}^{\alpha} r_{ij}^{\beta} B(\mathbf{r}_i, \mathbf{r}_j, \mathbf{R}) + m_i u_i^{\alpha} u_i^{\beta}\psi(\mathbf{r}_i - \mathbf{R})\right]_B. \tag{17}$$

Fig. 4(a) and (b) shows the virial and Hardy stress with enforced stoichiometry for CaO. Results for SiC and AlN are similar and are not shown. The fluctuation of the virial stress is considerably reduced and the convergence to the bulk stress value is much faster than using straight averages, shown in Fig. 3. However, the Hardy stress does not improve upon enforcing a stoichiometric average.

An alternative approach to improve the convergence of the local Hardy stress is to use localization functions that smoothly decay to zero at the surface of the spherical average volume. As discussed by Hardy [14] the localization functions

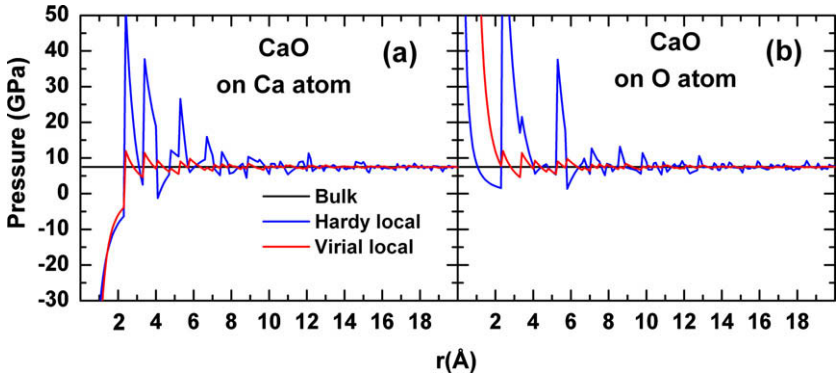

Fig. 4. Local stresses with enforced stoichiometry calculated at $T = 0$ K and 5% volume reduction for CaO at the (a) Ca, and (b) O atomic positions.

are arbitrary as long as they follow the conditions listed above. Fig. 5 shows the three localization functions that are considered here. All of these are polynomials that decay exactly to zero at the spherical surface ($x = |\mathbf{r} - \mathbf{R}|/r_c = 1$) and therefore have an exact normalization factor. The un-normalized functions are given below and include a linear, a cubic and a 7th order polynomial that has a functional form close to the Gaussian curve

(i) linear:

$$\psi(x) = 1 - x; \tag{18}$$

(ii) cubic:

$$\psi(x) = \frac{1}{2} - \frac{3}{2}\left(x - \frac{1}{2}\right) + 2\left(x - \frac{1}{2}\right)^3; \tag{19}$$

(iii) 7th order polynomial:

$$\psi(x) = (1 - x^2)^2\left[\frac{1}{2} - \frac{3}{2}\left(x - \frac{1}{2}\right) + 2\left(x - \frac{1}{2}\right)^3\right]. \tag{20}$$

The exact form of the smoothly decaying localization function is not critical, but its form does affect the convergence and the smoothness of the local stress as discussed below. The localizations functions were chosen to be general and independent functions with an easy calculation form for computational convenience.

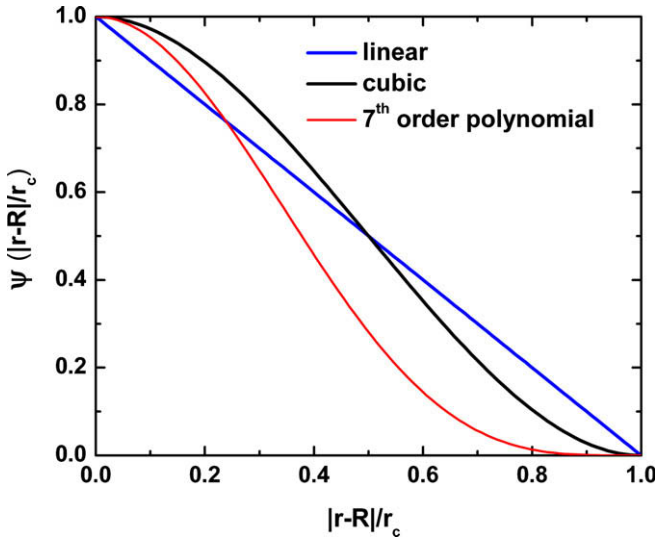

Fig. 5. Un-normalized polynomial localization functions used to improve convergence of spatial averages.

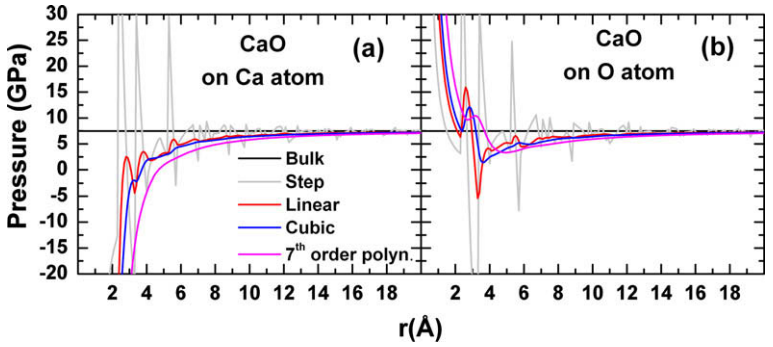

Fig. 6. Hardy local stress calculated for CaO at $T = 0$ K and 5% volume reduction using linear, cubic and 7th order polynomial localization functions.

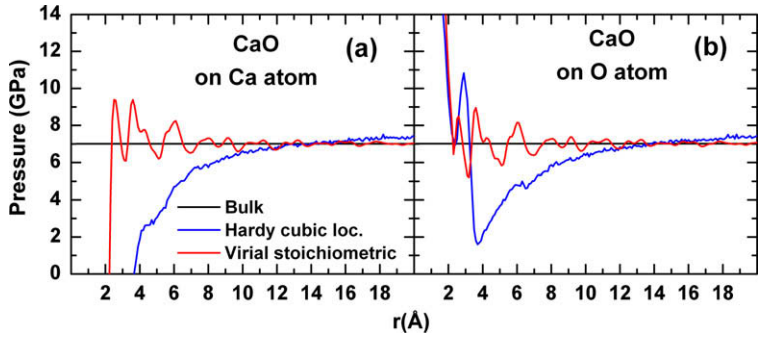

Fig. 7. Local stresses for CaO calculated at $T = 1000$ K at the same original density of the system at $T = 0$ K. Stoichiometric averaging is enforced in the virial and the cubic localization function is used in the Hardy local stress.

Fig. 6(a) and (b) shows the Hardy stress for the CaO calculated with these smoothly decaying localization functions compared to the Hardy stress with the step function used previously. The fluctuation of the Hardy local stress is considerably smoother at all radii for the smoothly decaying localization functions examined. However, the value of the calculated stress still converges slowly to the correct bulk value. As it is shown, in order to get within 20% deviation of the correct value, the local stress should be averaged with a radius of over 8 Å.

The effects of temperature and thermal fluctuations on the local stress calculations are investigated by calculating the virial and Hardy stresses for CaO at $T = 1000$ K in an MD simulation. As the volume is hold fixed at its $T = 0$ K value, the increase in temperature creates a positive pressure (the coefficient of thermal expansion is positive for these materials over this temperature range). For CaO, the resulted pressure is $\sim$7 GPa. As the system is not static, the local stress at each atomic position oscillates because of thermal fluctuations. To smooth out these fluctuations and to get a statistically meaningful quantity, the stress averages are performed over 10,000 time steps after the system reaches thermodynamic equilibrium. To make a fair comparison between the two methods, based on the results shown in Figs. 4 and 6, we used the best approachs so far, i.e., virial with enforced stoichiometry and the Hardy with the cubic localization function. Fig. 7(a) and (b) shows that the virial converges quicker to the correct bulk value than the Hardy stress. In particular, the virial stress deviation is within 25% at the first atomic shell at 2.4 Å while the Hardy stress only reaches this deviation at 6 Å. Therefore, the local stress calculated with the virial method with enforced stoichiometry clearly outperforms that calculated with the Hardy method using the cubic localization function.

4. Reducing fluctuations in small volume averages

4.1. Local density fluctuation

The fluctuations of thermodynamic quantities, averaged at atomic scales, have in fact many sources, largely related to the dynamic motion at finite temperatures, demanding space and time averages to reach physically meaningful quantities. Addressing the effect of these fluctuations on the local stress in small average volumes can be complicated. It is useful to evaluate the fluctuation in other local material properties. Particularly, the evaluation of the fluctuation of the local density may provide insight into fluctuations in the local pressure. It suggests that the fluctuations on the atomic scale are intrinsically related to the discreteness of the atomic structure and hence the choice of averaging volume has a large impact on the local quantities calculated. To illustrate this effect, we calculate the local density for the static structures of CaO, SiC and AlN;

see Fig. 8(a–c). These plots show that even at 10 Å the average density still shows a 5–13% deviation from the bulk average and, like the stress, the curve converges slowly. This suggests that fluctuation in any volume averaged atomic quantity is intrinsic and associated with the discreteness of the system. This is likely the major source of the fluctuations in the local virial stress for small average volumes. In order to reduce this intrinsic fluctuation we use two approaches, i.e. the localization functions employed in the Hardy local stress and the atomic voronoi volume.

4.2. Local density with localization functions

The idea of the Hardy localization functions is to spread the contribution of an individual atom into a region that is nearby. In the original formulation, Hardy used the step localization function. This makes the local density using localization functions given by Eq. (5) be equivalent to the straight average, N/V, which was performed previously and is shown in Fig. 8. With the use of the smoothly decaying localization functions shown in Fig. 5, we recalculate the local density for increasing radius and the results are shown in Fig. 9. The value of the bulk density and that of the straight average are also shown for reference. Only results for the CaO structure are shown but the conclusions are valid for the SiC and AlN structures. The fluctuation is considerably reduced using the smoothly decaying localization functions and the density converges quicker to the bulk value. From the three choices tested, the 7th order polynomial provides the best convergence. By the third atomic shell at 4.1 Å the local density deviation from the bulk value is less than 2%. We also perform a calculation of the local density in the dynamic case with $T = 1000$ K, making averages over 10,000 time steps in a MD simulation. The results are shown in Fig. 10 and besides some smoothing, the curves are essentially the same as those in Fig. 9.

4.3. Local density with voronoi atomic volume

The voronoi atomic volume is by definition the volume enclosing the space that is closer to a given atom than any other atom in an atomic structure [23,24]. While computationally demanding in the general case, the voronoi tessellation can be readily calculated in MD using efficient computational algorithms [25], taking advantage of the neighbor list generated for the force calculation. With the voronoi atomic volume, it is possible to define an atomic density, for each individual atom in the structure. The idea is not new and has been applied to the estimation of the density of proteins [26]. Except for atoms at a free surface, the voronoi volume is a unique, mathematically defined quantity. The density in a given volume can therefore

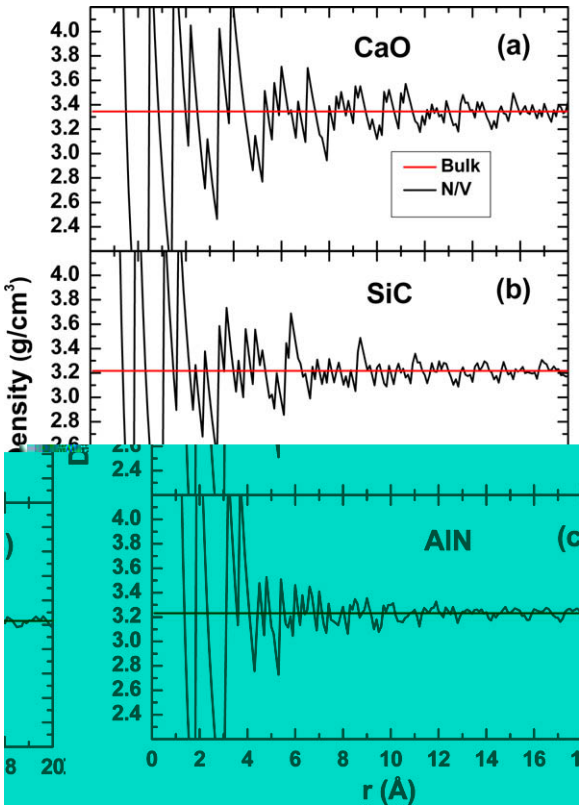

Fig. 8. Local densities calculated in a spherical volume centered in an atomic position for increasing radius for the static: (a) CaO, (b) SiC, and (c) AlN structures.

be calculated as the average of the atomic densities of the atom inside that volume. The voronoi local density for static structures gives exactly the bulk value at any average spherical radius as the atomic density is exactly N/V. Fig. 11 shows that the local density based on the voronoi atomic volumes provides the most accurate method of calculating the local density at

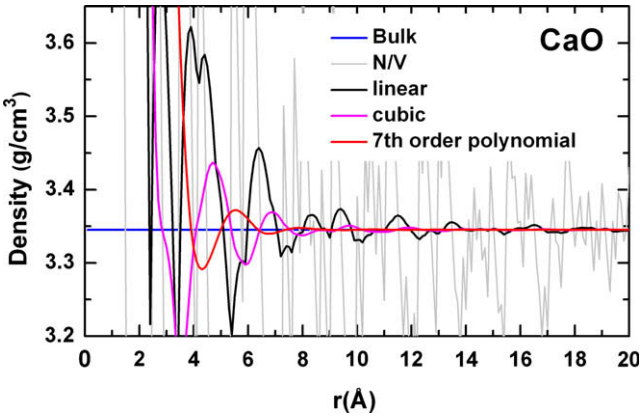

Fig. 9. Local densities for CaO static structure using localization functions compared to direct N/V and bulk densities.

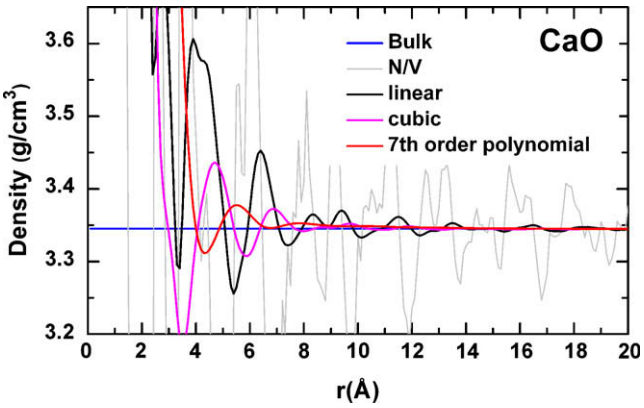

Fig. 10. Local densities for CaO structure at $T = 1000$ K. Averages are performed over 10,000 time steps in thermodynamic equilibrium.

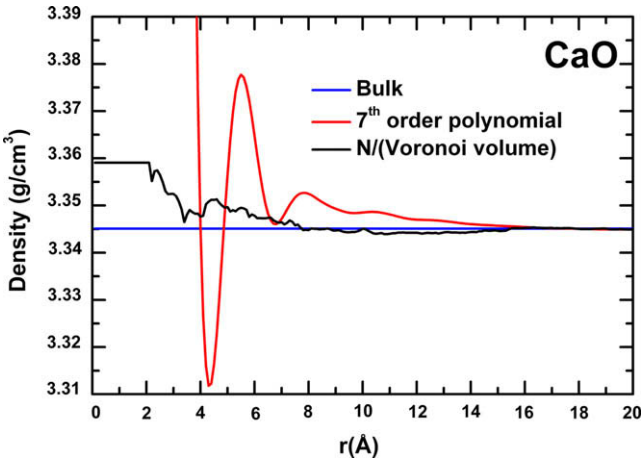

Fig. 11. Local densities for CaO at $T = 1000$ K. The direct density N/V is compared to the density calculated using the Voronoi atomic volume and using the 7th order polynomial localization function. Averages are done over 10,000 time steps in thermodynamic equilibrium.

finite temperature. The maximum deviation from the bulk value after averaging over 10,000 time steps is about 0.4%. Fig. 11 also shows the accurate local density obtained using the 7th order polynomial localization function for comparison.

5. Virial local stress with voronoi atomic volume and localization functions

Following the reduction of the fluctuation of the local density with the application of localization functions and the voronoi atomic volume, we attempt to reduce the fluctuation of the local stress using similar methods. We use three new expressions for the local virial stress:

(i) Virial with localization functions:

$$\pi^{\alpha\beta}(\mathbf{R}) = -\sum_{i=1}^{N}\left[\frac{1}{2}\sum_{\substack{j=1\\ j\neq i}}^{N} f_{ij}^{\alpha} r_{ij}^{\beta} + m_i v_i^{\alpha} v_i^{\beta}\right]\psi(\mathbf{r}_i - \mathbf{R}); \tag{21}$$

(ii) Virial with voronoi atomic volume, instead of the spherical volume:

$$\pi^{\alpha\beta}(\mathbf{R}) = -\frac{1}{\Omega^c}\sum_{\substack{i=1\\ i\in\Omega^c}}^{N}\left[\frac{1}{2}\sum_{\substack{j=1\\ j\neq i}}^{N} f_{ij}^{\alpha} r_{ij}^{\beta} + m_i v_i^{\alpha} v_i^{\beta}\right], \tag{22}$$

where Ω^c is the voronoi volume calculated by the sum of all the atomic voronoi volumes of the atoms inside the spherical volume of radius r_c centered at **R**.

(iii) Virial with enforced stoichiometry and voronoi atomic volume:

$$\pi^{\alpha\beta}(\mathbf{R}) = -\frac{m+n}{(k+l)\Omega^c}\left(k\pi_{Ca}^{\alpha\beta} + l\pi_{O}^{\alpha\beta}\right), \tag{23}$$

where Ω^c is the voronoi volume and the partial stresses are given by Eqs. (13) and (14).

Fig. 12(a) and (b) shows the virial local stress with the application of localization functions using Eq. (21) for the CaO structure at $T = 0$ K and 5% volume reduction. The large stress fluctuations shown in Fig. 3(a) and (b) for the stress calculated using the original virial expression are reduced and the stress converges quickly to the bulk stress value. The level of fluc-

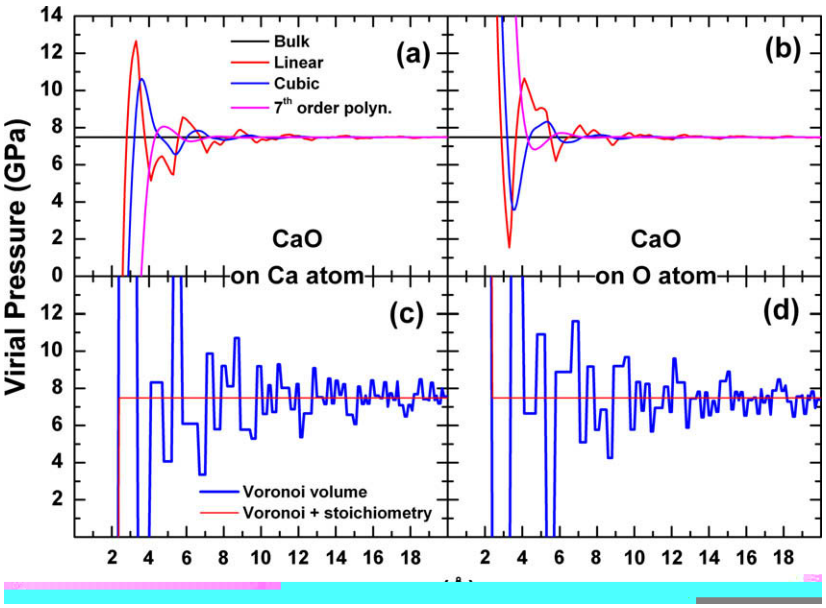

Fig. 12. Virial local stresses at $T = 0$ K and 5% volume reduction for CaO at Ca and O atoms. Linear, cubic and 7th order polynomial localization functions are used with no stoichiometric average in (a) and (b). Figures (c) and (d) show the effects of imposing the voronoi volume and stoichiometry constraint in addition to voronoi volume.

tuation obtained with the use of localization is comparable with the one obtained enforcing stoichiometry in the stress average, see Fig. 4(a) and (b).

Fig. 12(c) and (d) shows the local stress calculated using the Eqs. (22) and (23), making use of voronoi atomic volumes. The use of the voronoi volume instead of the spherical volume actually reduces significantly the fluctuation on the local stress, see Fig. 3(a) and (b). However, the convergence to the bulk stress values continues to be slow and compared with the reduction obtained with the use of localization functions the result is by far inferior. In the case of the application of the Eq. (23) assuming stoichiometric average and voronoi atomic volume the result is staggering since the local stress at the first atomic shell, at 2.4 Å in the case of CaO, gives the exact bulk stress value as can be seen in Fig. 12(c) and (d). Therefore, if the assumption of stoichiometry is reasonable, Eq. (23) offers by far the best method for the calculation of the local stress. In the general case, not assuming stoichiometry, Eq. (21) offers the best convergence and reduced fluctuations of the local stress compared to the original expression.

As a final test we calculate the local stress for a homogeneous sheared system. Fig. 13(a–d) shows the σ_{23} component of the local stress at $T = 0$ K and $\varepsilon_{23} = 0.05$. As in Fig. 12 the panels (a and b) show stresses with the application of localization functions while the panels (c and d) show stresses with the application of voronoi volumes with and without stoichiometric average. The results shown in Fig. 13 are consistent with those shown in Fig. 12 and demonstrate that the application of the techniques discussed for the calculation of the virial pressure are also valid for the calculation of shear stresses.

While the above analysis focused upon homogeneous deformation results, we briefly consider the inhomogeneous case by calculating the local stress distribution around an edge dislocation. Fig. 14(a–l) shows the local pressure calculated using several of the methods discussed in the text for an edge dislocation in CaO at $T = 0$ K and $P = 0$ GPa. For each method the local pressure is averaged over: 2.9 Å, midway between the first and second atomic shell; 4.45 Å, midway between the third and fourth atomic shell; and 7.5 Å, at the radius cut of the CaO interatomic potential. Fig. 14(a–c) shows the original virial and illustrate its large fluctuations even at 7.5 Å. The difference in pressure values at neighbor atoms is several GPas at all the three average radii in agreement with the curves shown in Fig. 2(a) and (b). Fig. 14(d–f) shows the Hardy stress with a cubic localization function. Like for the virial stress, the Hardy stress shows poor averages for the three radii. In agreement with the data in Fig. 6, the pressure difference for different components is several GPas at 2.9 Å and it is underestimated for 4.45 Å and 7.5 Å. Fig. 14(g–i) shows the virial stress with a 7th order polynomial localization function. As demonstrated by Fig. 12(a) and (b), the fluctuation at 2.9 Å is very large and the pressure values are very different between the two components. However, the pressure distribution at 4.45 Å and 7.5 Å are smooth and physically meaningful, correctly showing the compressive and tensile regions around the dislocation core. Fig. 14(j–l) shows the virial stress distribution calculated enforcing stoichiometry and making use of voronoi atomic volumes. As expected, the pressure distribution shown is smooth and physically meaningful at all radii, even at 2.9 Å. While the pressure distributions around the edge dislocation is reasonable (showing tension above the slip plane and compression below it), the pressure field is not perfectly symmetric about the slip plane, as expected based on linear elastic theory for an edge dislocation in an infinite medium. This small deviation from perfect symmetry has two main origins. First, the core of the edge dislocation in CaO is not symmetric and shows some extension in the direction normal to the slip plane, note the open space at the core above the slip plane. Second, the simulation cell has free

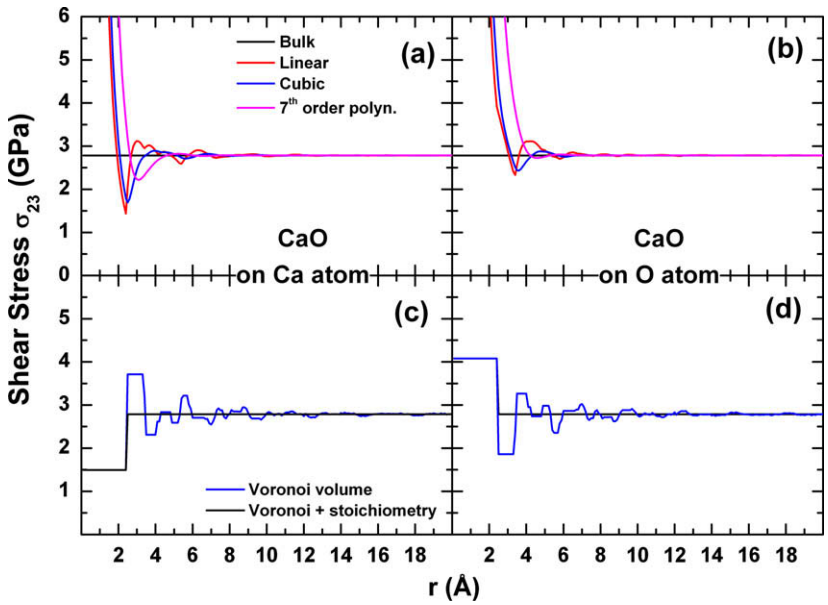

Fig. 13. σ_{23} shear local stresses at $T = 0$ K and $\varepsilon_{23} = 0.05$ for CaO at Ca and O atoms. Linear, cubic and 7th order polynomial localization functions are used with no stoichiometric average in (a) and (b) and voronoi volume with and without stoichiometry constraint are used in (c) and (d).

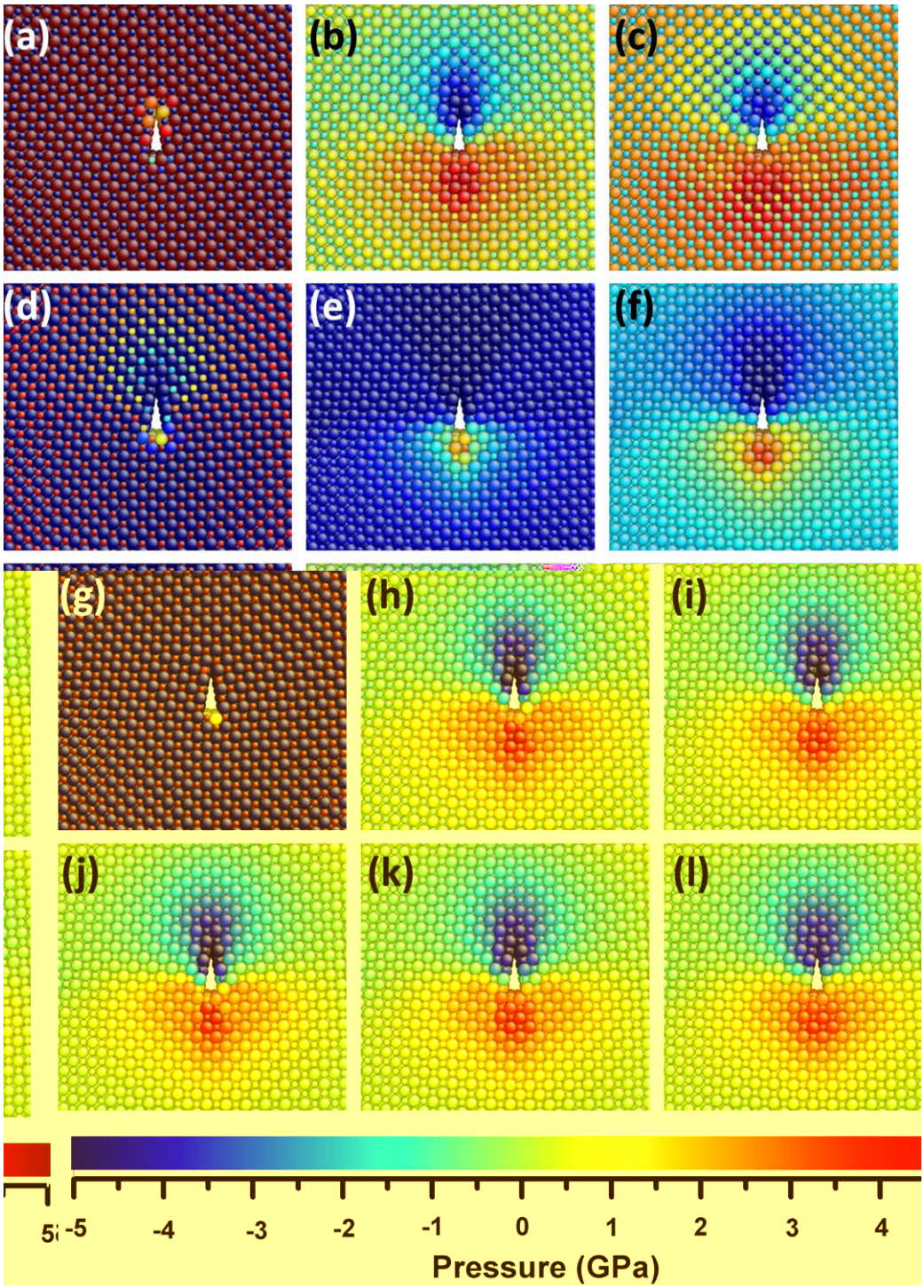

Fig. 14. Local pressure distribution around an edge dislocation core in CaO at $P = 0$ GPa and $T = 0$ K. The three columns show spherical averages over: 2.9 Å, 4.45 Å, and the potential radius cut 7.5 Å. The rows show the stress calculated using: (a–c) virial; (d–f) Hardy; (g–i) virial with 7th order polynomial localization function; (j–l) virial with Voronoi atomic volume and stoichiometric enforcement.

surfaces (rather than being an infinite medium) in the directions perpendicular to the dislocation line direction (it is periodic along the line direction). One of the free surfaces has a slip step, associated with the process used to produce the dislocation. The presence of a slip step and the difference in simulation cell width above and below the slip in the direction parallel to the Burgers vector also adds to the observed asymmetry in the pressure field with respect to the slip plane.

6. Conclusions

This paper discusses the calculation of the local atomic-level stress for multicomponent systems based on the virial and Hardy methods. It is shown that both methods provide local stress measures that converge slowly to bulk values in homogeneously strained systems. It is shown that the stress fluctuation is largely due to broken stoichiometry in the small averaging volume. Enforcing stoichiometric averaging considerably improves the convergence of the virial stress but has no effect on the convergence of the Hardy stress. Independent of the stress expression itself, it is shown that the fluctuation of local stress is also directly related to the fluctuation in the local density. It is demonstrated that this fluctuation can be reduced with the use of localizations functions, or completely eliminated when the voronoi atomic volume is used. Redefining the enforced stoichiometric virial to use voronoi atomic volumes makes it converge to the correct bulk stress value by the first atomic shell, at 2.4 Å for CaO. However, assuming stoichiometry may be questionable close to defects such as grain boundaries. In that case, the virial stress using localization functions is shown to provide a computational affordable alternative that converges quickly to the bulk value, e.g., the stress value by the third atomic shell, at 4.1 Å for CaO, deviates from the bulk values by less than 7%. These results highlight the accuracy of the proposed redefined virial expressions for the calculation of local stress. It is demonstrated that they consistently converge faster than the Hardy local stress. This conclusion contrasts with those in other recent work [18] where comparisons between the original virial expression and the Hardy expression favor the latter. The virial-based local stress is convenient in that it can be evaluated within the main MD loop with little computational effort. On the other hand, the Hardy expression requires an additional loop over each atomic position in order to calculate the bond function term. All the calculations here are done for binary systems but the results are valid for a general multicomponent system, which includes the single component case. The results are also independent on the type of atomic interaction and valid for any many body interatomic potential. Therefore, the redefined virial expressions using enforced stoichiometry and voronoi volumes or localization functions are shown to be accurate and computationally affordable methods for the calculation of local stresses in the general case.

References

[1] R.W. Smith, D.J. Srolovitz, J. Appl. Phys. 79 (1996) 1448.
[2] C. Zhang, R.K. Kalia, A. Nakano, P. Vashishta, P.S. Branicio, J. Appl. Phys. 103 (2008) 083508.
[3] P.S. Branicio, R.K. Kalia, A. Nakano, P. Vashishta, Phys. Rev. Lett. 96 (2006) 065502.
[4] P.S. Branicio, R.K. Kalia, A. Nakano, P. Vashishta, F. Shimojo, J.P. Rino, J. Mech. Phys. Solid 56 (2008) 1955.
[5] H. Tsuzuki, P.S. Branicio, J.P. Rino, Appl. Phys. Lett. 92 (2008) 191909.
[6] H. Tsuzuki, P.S. Branicio, J.P. Rino, Acta Mater. 57 (2009) 1843.
[7] M.E. Bachlechner, A. Omeltchenko, A. Nakano, R.K. Kalia, P. Vashishta, I. Ebbsjo, A. Madhukar, P. Messina, Appl. Phys. Lett. 72 (1998) 1969.
[8] M.A. Makeev, A. Madhukar, Phys. Rev. Lett. 86 (2001) 5542.
[9] R.J.E. Clausius, Phil. Mag. 40 (1870) 122.
[10] J.C. Maxwell, Trans. R. Soc. Edinb. 26 (1870) 1.
[11] J.C. Maxwell, Nature 10 (1874) 477.
[12] D.H. Tsai, J. Chem. Phys. 70 (1979) 1375.
[13] K.S. Cheung, S. Yip, J. Appl. Phys. 70 (1991) 5688.
[14] R.J. Hardy, J. Chem. Phys. 76 (1982) 622.
[15] J.F. Lutsko, J. Appl. Phys. 64 (1988) 1152.
[16] J.H. Irving, J.G. Kirkwood, J. Chem. Phys. 18 (1950) 817.
[17] S. Root, R.J. Hardy, D.R. Swanson, J. Chem. Phys. 118 (2003) 3161.
[18] J.A. Zimmerman, E.B. Webb, J.J. Hoyt, R.E. Jones, P.A. Klein, D.J. Bammann, Model. Simulat. Mater. Sci. Eng. 12 (2004) S319.
[19] T.J. Delph, Model. Simulat. Mater. Sci. Eng. 13 (2005) 585.
[20] Y.P. Chen, J. Chem. Phys. 124 (2006) 054113.
[21] R.C. Mota, P.S. Branicio, J.P. Rino, Europhys. Lett. 76 (2006) 836.
[22] P. Vashishta, R.K. Kalia, A. Nakano, J.P. Rino, J. Appl. Phys. 101 (2007) 103515.
[23] W. Brostow, J.P. Dussault, B.L. Fox, J. Comput. Phys. 29 (1978) 81.
[24] J.L. Finney, J. Comput. Phys. 32 (1979) 137.
[25] M. Tanemura, T. Ogawa, N. Ogita, J. Comput. Phys. 51 (1983) 191.
[26] M.L. Quillin, B.W. Matthews, Acta Crystallogr. Sec. D – Biol. Crystallogr. 56 (2000) 791.